The Journal of Immunology

A Pathogenic Role for CD4$^+$ T Cells during Chikungunya Virus Infection in Mice

Teck-Hui Teo, Fok-Moon Lum, Carla Claser, Valeria Lulla, Aleksei Lulla, Andres Merits, Laurent Rénia and Lisa F. P. Ng

J Immunol 2013; 190:259-269; Prepublished online 3 December 2012;
doi: 10.4049/jimmunol.1202177
http://www.jimmunol.org/content/190/1/259

The Journal of Immunology is published twice each month by
The American Association of Immunologists, Inc.,
1451 Rockville Pike, Suite 650, Rockville, MD 20852

Print ISSN: 0022-1767 Online ISSN: 1550-6606.

A Pathogenic Role for CD4$^+$ T Cells during Chikungunya Virus Infection in Mice

Teck-Hui Teo,*,†,[1] Fok-Moon Lum,*,‡,[1] Carla Claser,* Valeria Lulla,§ Aleksei Lulla,§ Andres Merits,§ Laurent Rénia,*,[2] and Lisa F. P. Ng*,‡,[2]

Chikungunya virus (CHIKV) is an alphavirus that causes chronic and incapacitating arthralgia in humans. Injury to the joint is believed to occur because of viral and host immune-mediated effects. However, the exact involvement of the different immune mediators in CHIKV-induced pathogenesis is unknown. In this study, we assessed the roles of T cells in primary CHIKV infection, virus replication and dissemination, and virus persistence, as well as in the mediation of disease severity in adult RAG2$^{-/-}$, CD4$^{-/-}$, CD8$^{-/-}$, and wild-type CHIKV C57BL/6J mice and in wild-type mice depleted of CD4$^+$ or CD8$^+$ T cells after Ab treatment. CHIKV-specific T cells in the spleen and footpad were investigated using IFN-γ ELISPOT. Interestingly, our results indicated that CHIKV-specific CD4$^+$, but not CD8$^+$, T cells are essential for the development of joint swelling without any effect on virus replication and dissemination. Infection in IFN-γ$^{-/-}$ mice demonstrated that pathogenic CD4$^+$ T cells do not mediate inflammation via an IFN-γ–mediated pathway. Taken together, these observations strongly indicate that mechanisms of joint pathology induced by CHIKV in mice resemble those in humans and differ from infections caused by other arthritogenic viruses, such as Ross River virus. ***The Journal of Immunology*****, 2013, 190: 259–269.**

Chikungunya virus (CHIKV) is a re-emerging arbovirus endemic to Africa, India, and many parts of Asia (1). Since 2004, circulation of CHIKV has been increasing, with massive outbreaks affecting millions in the Indian Ocean islands and Southeast Asia (2–5). Currently, sporadic outbreaks continue in various endemic countries (6, 7).

CHIKV is an arthropod-borne alphavirus transmitted primarily by *Aedes* mosquitoes, namely *Aedes aegypti* and *Aedes albopictus* (8). The hallmark of CHIKV infection is polyarthralgia, with patients having joint pain and inflammation (9). Other classical symptoms of CHIKV infection include febrile illness (temperature usually >38.9°C), maculopapular rashes, myalgia, headache, edema of the extremities, and gastrointestinal complaints (10, 11). In some cases, CHIKV complications, such as acute nephritis (12), myocarditis, pericarditis (13), myopericarditis (14), retrobulbar neuritis (15), neurologic complications, and death, have also been reported (16, 17).

Currently, CHIKV pathogenesis remains poorly defined. Most studies have focused extensively on host innate immunity against the virus, particularly type I IFN and related pathways (18–23). Although these studies demonstrated the importance of type I IFN in controlling virus replication during early infection, its effects are inadequate for complete virus clearance and result in virus persistence in the tissues. In both macaque and mouse models, CHIKV was reported to persist consistently in tissues and organs even after viremia has subsided and the levels of IFN-α/β have returned to normal (20, 24). These observations support the hypothesis that adaptive immunity plays an important role in the elimination of virus persistence after IFN-α/β responses have subsided.

Our current understanding of T cell involvement during CHIKV infection is at the nascent stage. An increase in the fraction of activated peripheral T cells during acute CHIKV infection was reported in two clinical studies (25, 26). In a mouse model, it was shown that infiltration of CD4$^+$ and CD8$^+$ T cells occurred in the inflamed joint of CHIKV-infected animals (24, 27). Although these observations suggested an active participation of T cells during the symptomatic phase of CHIKV infection, the functional roles of T cells in the induction of disease pathology remain largely undefined.

To assess the roles of T cells in CHIKV infection, RAG2$^{-/-}$, CD4$^{-/-}$, and CD8$^{-/-}$ mice, as well as wild-type (WT) mice depleted of CD4$^+$ or CD8$^+$ T cells, were infected and monitored for CHIKV infection and replication, dissemination and joint pathology, and CHIKV-induced disease severity. In addition, the presence of CHIKV-specific T cells in the spleen and footpad were investigated. Our findings demonstrated that in situ CHIKV-induced joint swelling is mediated by infiltration of CHIKV-specific CD4$^+$ T cells that do not have any apparent antiviral role. Furthermore, CD8$^+$ T cells did not have any role in antiviral response or pathology during CHIKV infection. Lastly, infection in IFN-γ$^{-/-}$ mice demonstrated that CD4$^+$ T cells do not mediate joint swelling via an IFN-γ–mediated pathway.

*Singapore Immunology Network, Agency for Science, Technology and Research, Biopolis, Singapore 138648; †National University of Singapore Graduate School for Integrative Sciences and Engineering, National University of Singapore, Singapore 117456; ‡Department of Biochemistry, Yong Loo Lin School of Medicine, National University of Singapore, Singapore 117597; and §Institute of Technology, University of Tartu, 50411 Tartu, Estonia

[1]T.-H.T. and F.-M.L. contributed equally to this work.

[2]L.R. and L.F.P.N. directed this work equally.

Received for publication August 6, 2012. Accepted for publication October 25, 2012.

This work was supported by core grants from the Singapore Immunology Network and the Horizontal Programme on Infectious Diseases, Agency for Science, Technology and Research, Singapore. Part of this work was also supported by the European Union FP7 project: Integration of Chikungunya Research "ICRES" Grant 261202. F.-M.L. is supported by a National University of Singapore postgraduate scholarship, and T.-H.T. is supported by an Agency for Science, Technology and Research postgraduate scholarship.

Address correspondence and reprint requests to Dr. Lisa F.P. Ng and Dr. Laurent Rénia, Singapore Immunology Network, Agency for Science, Technology and Research, Immunos, 8A Biomedical Grove, Biopolis, Singapore 138648. E-mail addresses: lisa_ng@immunol.a-star.edu.sg (L.F.P.N.) and renia_laurent@immunol.a-star.edu.sg (L.R.)

The online version of this article contains supplemental material.

Abbreviations used in this article: CHIKV, Chikungunya virus; dpi, days postinfection; Fluc, firefly luciferase; FOV, field of view; FOV-C, field of view for the foot; FOV-D, field of view for the whole body; WT, wild-type.

Materials and Methods

Mice

Female WT, RAG2$^{-/-}$, CD4$^{-/-}$, CD8$^{-/-}$, and IFN-$\gamma^{-/-}$ C57BL/6J mice were used. All mice were 6 wk old and were bred and kept under specific pathogen–free conditions in the Biopolis Resource Center, Singapore. Age- and sex-matched WT and deficient mice were used in all experiments. All experiments and procedures using mice were approved by the Institutional Animal Care and Use Committee (IACUC: 080383) of the Agency for Science, Technology and Research in accordance with the guidelines of the Agri-Food and Veterinary Authority and the National Advisory Committee for Laboratory Animal Research of Singapore.

Virus

CHIKV strain SGP11 was isolated from an outbreak in Singapore and maintained in Vero-E6 cells, as previously described (21). Viruses were further propagated in C6/36 cells and purified by ultracentrifugation (28) prior to their use for in vivo infections. Virus titer was determined by standard plaque assays using Vero-E6 cells (21). A CHIKV variant, expressing the firefly luciferase (Fluc) was constructed using a full-length infectious cDNA clone of CHIKV LR2006-OPY1 isolate (29). Briefly, the infectious cDNA was cloned into a modified pMA vector (GeneArt, Regensburg, Germany) with an SP6 promoter upstream of 5′ of CHIKV cDNA. Sequencing was conducted to ensure that no mutations were introduced. A Fluc insert was introduced at 5′ to the structural genes of infectious cDNA clone, followed by duplication of a second subgenomic promoter, as described (30). Infectious viruses were rescued from infectious cDNA clones in BHK 21 cells, as described (29), followed by propagation and titration in C6/36 cells. Viruses were purified by ultracentrifugation prior to their use for in vivo infection, and titer was determined using standard plaque assays with Vero-E6 cells (21, 28).

Virus infection and evaluation of disease

Mice were inoculated s.c. in the ventral side of the right hind footpad toward the ankle with 1×10^6 PFU CHIKV in 50 μl PBS. Viremia was monitored daily beginning at 24 h postinfection and lasting until 8 d postinfection (dpi), and subsequently on every alternate day until 14 dpi. Foot swelling was quantified daily from 0 to 14 dpi, as previously described (28). Measurements were done for both height (thickness) and breadth of the foot and were quantified as (height × breadth). The degree of swelling was expressed as the relative percentage increase in footpad size compared with preinfection (day 0), using the following formula: $[(x - \text{day } 0)/\text{day } 0 \times 100]$, where x is the quantified footpad measurement for each respective day.

Viral RNA extraction and viral copies quantification

Ten microliters of blood was collected from the tail vein. Samples were diluted in 120 μl PBS and 10 μl citrate-phosphate-dextrose solution (Sigma-Aldrich). Viral RNA extractions were subsequently done using a QIAamp Viral RNA Kit (QIAGEN), following the manufacturer's instructions. Viral copies were quantified by quantitative RT-PCR using a QuantiTect Probe RT-PCR Kit (QIAGEN), as previously described (28).

In vivo imaging

Virus replication and dissemination were assessed daily from 1 to 8 dpi, subsequently on every alternate day until 30 dpi, and every 5 d until 65 dpi by bioluminescence signals using an in vivo bioluminescence imaging system (IVIS Spectrum; Xenogen, Alameda, CA). Luciferase substrate, D-luciferin potassium salt (Caliper Life Sciences), was dissolved in PBS at a concentration of 5 mg/ml. Mice were shaved and anesthetized in an oxygen-rich induction chamber with 2% isoflurane. Measurements were performed 2 min after s.c. injection of 100 μl luciferin solution. Whole-body imaging was performed with the animal in a ventral position. Foot imaging was performed with the animal in a dorsal position. Bioluminescence imaging was acquired with a field of view (FOV) of 21.7 and 13.1 cm for the whole body (FOV-D) and foot (FOV-C), respectively. Exposure condition was an initial 60 s, followed by a 4-min delay and another exposure at 60 s. In the event that luminescence readings were above the detection limit of the machine, the exposure time was reduced and kept consistent across groups. Bioluminescence signals taken preinfection (0 dpi) were used for background subtraction. For bioluminescence quantifications, regions of interest were drawn using the Living Image 3.0 software, and the average radiance (p/s/cm^2/sr) was determined.

In vivo T cell depletion

Purified rat IgG2b anti-mouse CD4 (clone GK1.5) and rat IgG2a anti-mouse CD8 (clone YTS 169.4; both from Bio X Cell) mAbs were used to deplete CD4$^+$ and CD8$^+$ T cells, respectively. In the early-depletion groups, 500 μg depleting Abs was injected i.p. on −1 and 4 dpi. For the late-depletion groups, 500 μg depleting Abs was injected i.p. on 4 dpi (before the onset of inflammation). Control mice received 500 μg purified rat IgG (Sigma-Aldrich) i.p. at −1 and 4 dpi. Depletion efficiencies were verified by flow cytometry using Abs recognizing epitope specificities other than those recognized by depleting Abs at 0 dpi (before infection) and at 10 dpi and were always >95%. Briefly, 10 μl blood was mixed with 10 μl EDTA/PBS (10 μM). RBCs were lysed with RBC lysis buffer (R&D Systems) and incubated at room temperature for 10 min. Cells were centrifuged at 500 × *g*. Supernatant was removed, and cells were resuspended in 100 μl blocking buffer consisting of a mix of 1% rat serum and mouse serum (both from Sigma-Aldrich) in FACS buffer (PBS + 3% FBS; Life Technologies) and incubated for 5 min. Next, cells were stained with PE-Cy7–conjugated anti-mouse CD45 (clone 30-F11; BD Biosciences), FITC-conjugated anti-mouse CD3 (clone 145-2C11; BD Biosciences), Pacific Blue–conjugated anti-mouse CD4 (clone GK1.5; BioLegend), and allophycocyanin-conjugated anti-mouse CD8 (clone 53-6.7; BD Biosciences) Abs for 20 min at room temperature before the addition of 300 μl FACS buffer. Data were acquired using an LSR II flow cytometer (BD Biosciences) with FACSDiva software and analyzed using FlowJo (v7.6) software.

Ex vivo depletion of CD4$^+$ T cells

A total of 2×10^7 splenocytes and 3×10^6 cells from the feet of CHIKV-infected and naive mice was subjected to CD4$^+$ T cell positive depletion using a MACS column loaded with anti-mouse CD4 microbeads, according to the manufacturer's instructions (Miltenyi Biotec). Efficiency of depletion was >99% and ∼70% in the spleen and joints, respectively, as verified by flow cytometry.

Histology

Mice were perfused by intracardial injection with PBS, and foot tissues were removed and fixed with 4% paraformaldehyde. Fixed tissues were embedded in paraffin wax, processed to obtain 5-μm sections, and subjected to H&E staining following established protocols.

Spleen and hind feet joint cell isolation

Mice were infected, and spleens were harvested at different times post-infection. Spleens were dissociated in RPMI 1640 medium containing 10% FBS (complete RPMI). After passing through a 40-μm cell strainer, the cells were collected and centrifuged at 500 × *g* for 5 min. RBCs were lysed by osmotic shock using buffered ammonium chloride solution. Cells were washed once with complete RPMI medium, and splenocytes were resuspended in 10 ml complete RPMI medium. Cell viability, always >95%, was assessed using trypan blue.

For the hind feet joint cell analysis, mice were sacrificed, and footpads and ankles were removed at 6 dpi, deskinned, and placed immediately in 4 ml digestion medium containing dispase (2 U/ml; Invitrogen), Collagenase IV (20 μg/ml; Sigma-Aldrich), and DNase I mix (50 μg/ml; Roche Applied Science) in complete RPMI medium. Tissues were incubated in digestion medium for 4 h at 37°C, 5% CO_2 on a shaker. Digested tissues and digestion medium were deposited onto a 40-μm cell strainer, and 3 ml fresh complete RPMI medium was added. Digested tissues were ground against the cell strainer with a 1-ml syringe plunger, using a circular motion to release a maximum number of cells into the medium. Cells were centrifuged at 500 × *g*, and RBCs were lysed in buffered ammonium chloride solution. Cells were washed once in complete RPMI medium, resuspended in 10 ml complete RPMI medium, and overlaid onto 10 ml 35% v/v Percoll/RPMI 1640 medium (Sigma-Aldrich). Cells were centrifuged at 2400 rpm for 20 min, resuspended, and washed once more with complete medium before being counted.

Phenotyping of leukocytes

Splenocytes and footpad cells were washed once in complete medium, and cell pellets were resuspended in 100 μl blocking buffer and incubated for 20 min. Staining was performed using allophycocyanin-Cy7–conjugated anti-CD45 (clone 30-F11; BD Biosciences), PE-Cy7–conjugated anti-CD3 (clone 145-2C11; BD Biosciences), PE-conjugated anti-CD4 (clone GK1.5, eBioscience), allophycocyanin-conjugated anti-CD8 (clone 53-6.7; BD Biosciences), FITC-conjugated anti-Ly6G (clone RB6-8C5; eBioscience), PerCP5.5-conjugated anti-CD11b (clone M1/70; eBioscience), and e450-conjugated anti-NK1.1 (clone PK136; eBioscience) Abs for 30 min at room temperature. Live cells were determined by final resuspension of stained cells in 500 μl DAPI (10 ng/ml) or with additional staining with a Live/Dead determination dye (Invitrogen) for 30 min before cell-specific marker staining. Data were acquired using an LSR II flow cytometer (BD Biosciences) with FACSDiva software and analyzed using

FlowJo software. The different leukocyte populations present in the footpad were identified and defined as described in Supplemental Fig. 1.

ELISPOT assay

Polyvinylidene difluoride membrane Multiscreen HTS-IP plates (Millipore) were humidified with 70% ethanol, washed, and coated overnight with 50 μl anti–IFN-γ capture Abs (clone AN18; Mabtech) per well. For in vivo depletion, mice were treated with 500 μg anti-mouse CD4 mAbs (clone GK1.5; Bio X Cell) at 5 dpi, whereas control mice received an i.p. injection of 500 μg rat IgG (Sigma-Aldrich). Mice were sacrificed on 6 dpi, and splenocytes and footpad cells were extracted as described above. For ex vivo depletion, extracted cells were subjected to $CD4^+$-depleting MACS column, as described above. A total of 300,000 splenocytes from infected mice (in 50 μl complete RPMI medium) from each sample was stimulated with 1.5×10^6 SGP11 virions in 50 μl complete RPMI medium

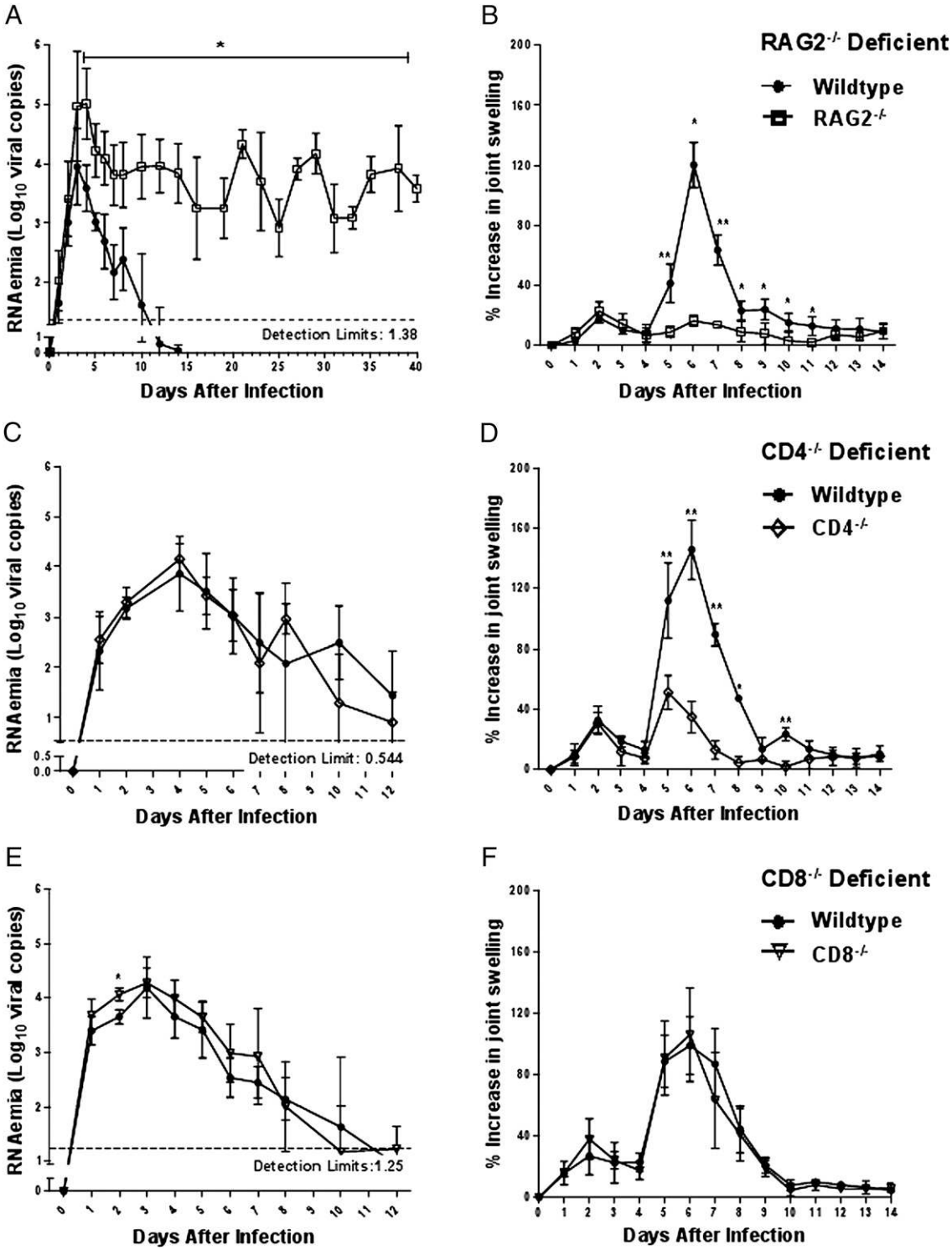

FIGURE 1. Joint swelling and CHIKV RNAemia in $RAG2^{-/-}$, $CD4^{-/-}$, and $CD8^{-/-}$ deficient mice. RNAemia (**A**) and percentage increase in joint swelling (**B**) in WT ($n = 7$) and $RAG2^{-/-}$ ($n = 4$) mice. RNAemia monitoring was terminated at 40 dpi. RNAemia (**C**) and percentage increase in joint swelling (**D**) in WT and $CD4^{-/-}$ mice ($n = 5$/group), respectively. RNAemia (**E**) and percentage increase in joint swelling (**F**) in WT and $CD8^{-/-}$ mice ($n = 5$/group). All groups were infected with CHIKV SGP11. Detection limits of RNAemia were determined by average signals from blood of mock-infected mice ($n = 2$). $^*p < 0.05$, $^{**}p < 0.01$, Mann–Whitney test.

containing 60 U/ml IL-2 (eBioscience). A total of 100,000 footpad cells (in 16.7 μl complete RPMI medium) and 200,000 splenocytes (in 33.3 μl complete RPMI medium) from naive mice was stimulated with 1.5×10^6 SGP11 virions in 50 μl complete RPMI medium containing 60 U/ml IL-2. Cells were stimulated with the Ag or with Con A (at a concentration of 10 μg/ml) as positive control, for 18 h at 37°C, 5% CO_2. Cells in complete RPMI medium containing 60 U/ml IL-2 without any Ag stimulation were used as negative control. After incubation, cells were removed, and wells were washed six times with 0.01% v/v PBS/Tween 20. Following that, 100 μl biotinylated anti–IFN-γ–detecting Ab (clone R4-6A2; Mabtech), at 2 μg/ml in PBS/0.5% BSA, was added to each well and incubated for 2 h at 37°C, 5% CO_2. Plates were then washed with 0.01% v/v PBS/Tween 20 to remove unbound Abs, and 100 μl extravidin–alkaline phosphatase (at 1:1000 dilution, Sigma-Aldrich) was added to each well and incubated for 45 min at room temperature. Plates were then washed with 0.01% v/v PBS/Tween 20, followed by PBS, to remove traces of Tween 20. Lastly, 75 μl BCIP/NBT (Sigma-Aldrich) was added to each well and incubated for 8 min before washing with water to stop the reaction. The number of spots was quantified using ImmunoSpot 5.0 Analyzer Professional DC software (Cellular Technology).

Statistical analysis

Data are presented as mean ± SD. Differences between groups and controls were analyzed using appropriate tests (Mann–Whitney *U* test, Kruskal–Wallis with Dunn posttest, one-way ANOVA with Tukey posttest). Statistics were performed with GraphPad Prism 5.04.

Results

Persistent viremia with no CHIKV-induced inflammation in RAG2$^{-/-}$ deficient mice

To uncover a functional role for the adaptive-immune response against CHIKV infection, adult RAG2$^{-/-}$ (with no B and T cells) C57BL/6J mice were injected in the footpad with 10^6 PFU of CHIKV SGP11. Infected RAG2$^{-/-}$ mice had a higher peak of RNAemia at 3–4 dpi, and it persisted at a high levels beyond 40 dpi, whereas RNAemia in WT C57BL/6J mice was resolved by 14 dpi (Fig. 1A). Interestingly, despite harboring a higher RNAemia, RAG2$^{-/-}$ mice had no signs of severe joint swelling. In contrast, maximum joint swelling was observed on 6 dpi in WT mice (Fig. 1B). However, a minor peak in swelling that occurred at 2 dpi in the WT mice was also observed in RAG2$^{-/-}$ mice. These results demonstrate that host adaptive immunity is required for controlling and eliminating the virus from the host and is mediating maximal CHIKV-induced swelling in the joints.

CHIKV infection in CD4$^{-/-}$ and CD8$^{-/-}$ deficient mice

We next attempted to decipher the roles of T cell subsets in CHIKV infection using CD4$^{-/-}$ and CD8$^{-/-}$ mice. Similar to previous experiments, both WT and deficient mice were infected with 1×10^6 PFU of CHIKV SGP11 in the footpad. RNAemia was identical in WT and deficient mice, indicating that these T cell subsets have no role in the control and elimination of CHIKV (Fig. 1C, 1E). The peak of joint swelling observed at 6 dpi was significantly reduced in the CD4$^{-/-}$ mice but not in the CD8$^{-/-}$ mice (Fig. 1D, 1F). In addition, H&E staining of swollen footpads revealed reduced polymorphonuclear cell infiltration and tissue damage in the muscles and tendons of CD4$^{-/-}$ mice compared with WT and CD8$^{-/-}$ mice (Fig. 2). Taken together, these data suggest that CD4$^+$ T cells mediate CHIKV-induced joint pathology.

CD4$^+$, but not CD8$^+$, T cells are responsible for mediating footpad inflammation

To further define the roles of CD4$^+$ and CD8$^+$ T cells, we next performed experiments with infected WT mice depleted of these subsets by Ab treatment. In addition, we made use of another CHIKV variant, an infectious cDNA clone of CHIKV LR2006-OPY1 isolate tagged with firefly luciferase (LR2006-OPY1-Fluc), allowing virus dissemination to be imaged (Figs. 3, 4). Infection with LR2006-OPY1-Fluc presented the same patterns of RNAemia and pathogenesis observed for CHIKV SGP11. However, with bioluminescence imaging, we observed that viral development in the joint was a swift process, with two maximum peaks of development at 12 and 3 dpi, respectively (Fig. 4C, 4D). A rapid reduction in the bioluminescent signal was observed between 5 and 6 dpi. Subsequently, a gradual reduction in the signal intensity occurred until recovery (Figs. 3C, 3D, 4C, 4D). This likely resulted from a decrease in viral gene expression and/or virus elimination. Surprisingly, imaging also revealed that virus persisted in the joint until 60 dpi (Figs. 3C, 3E, 4C, 4E), long after the clearance of RNAemia and joint swelling (Figs. 3A, 3B, 4A, 4B). Despite virus persistence, dissemination was minimal. The spread of inoculated LR2006-OPY1-Fluc was detected only by bioluminescence in the right thigh uniquely at 3 h postinfection, and virus spread from the site of injection was observed in the uninfected foot and tail between 1 and 4 dpi (Supplemental Fig. 2).

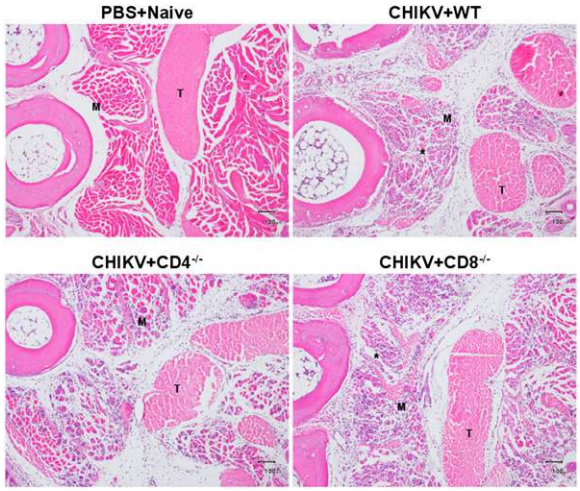

FIGURE 2. Reduction in joint pathology in CD4$^{-/-}$ mice. Representative histopathology photographs of swelling footpad in PBS+Naive, CHIKV +WT, CHIKV+CD4$^{-/-}$, and CHIKV+CD8$^{-/-}$ mice on 6 dpi. H&E staining and transverse sectioning was done. The asterisks denote regions of severe infiltration and tissue damage. Scale bars, 100 μm. M, Muscle; T, tendon.

In a first set of experiments, mice were treated with CD4-depleting Abs either at −1 and 4 dpi (early depletion) or only at 4 dpi just before the onset of the major peak of joint swelling (late depletion). Neither treatment had any effect on RNAemia (Fig. 3A), virus dissemination, or luciferase gene expression in the footpad (Fig. 3C, 3D). However, although the depletion of CD4$^+$ T cells significantly reduced the major peak of joint swelling seen at 5–6 dpi, it had no effect on the smaller peak that occurred at 1–2 dpi (Fig. 3B). Late depletion performed at 4 dpi, just before the onset of the major peak in swelling, was sufficient to reduce significantly the maximum joint swelling observed from 5–10 dpi (Fig. 3B). These results confirmed the earlier observations presented for the infection of CD4$^{-/-}$ mice with CHIKV SGP11 (Fig. 1C).

In a second series of experiments, mice were also treated with anti-CD8 Abs using the same protocol for CD4$^+$ T cell depletion. Expectedly, CD8$^+$ T cell depletion in WT mice had no effect on RNAemia, luciferase gene expression in the footpad, virus dissemination, or the development of joint swelling (Fig. 4). Collectively, these observations clearly suggest that joint swelling was mediated primarily by CHIKV-specific CD4$^+$ T cells.

CHIKV-specific CD4$^+$ T cells are present in the feet of mice during and after CHIKV infection

To demonstrate the presence of pathogenic CD4$^+$ T cells in the infected joints, leukocytes were isolated from CHIKV-infected

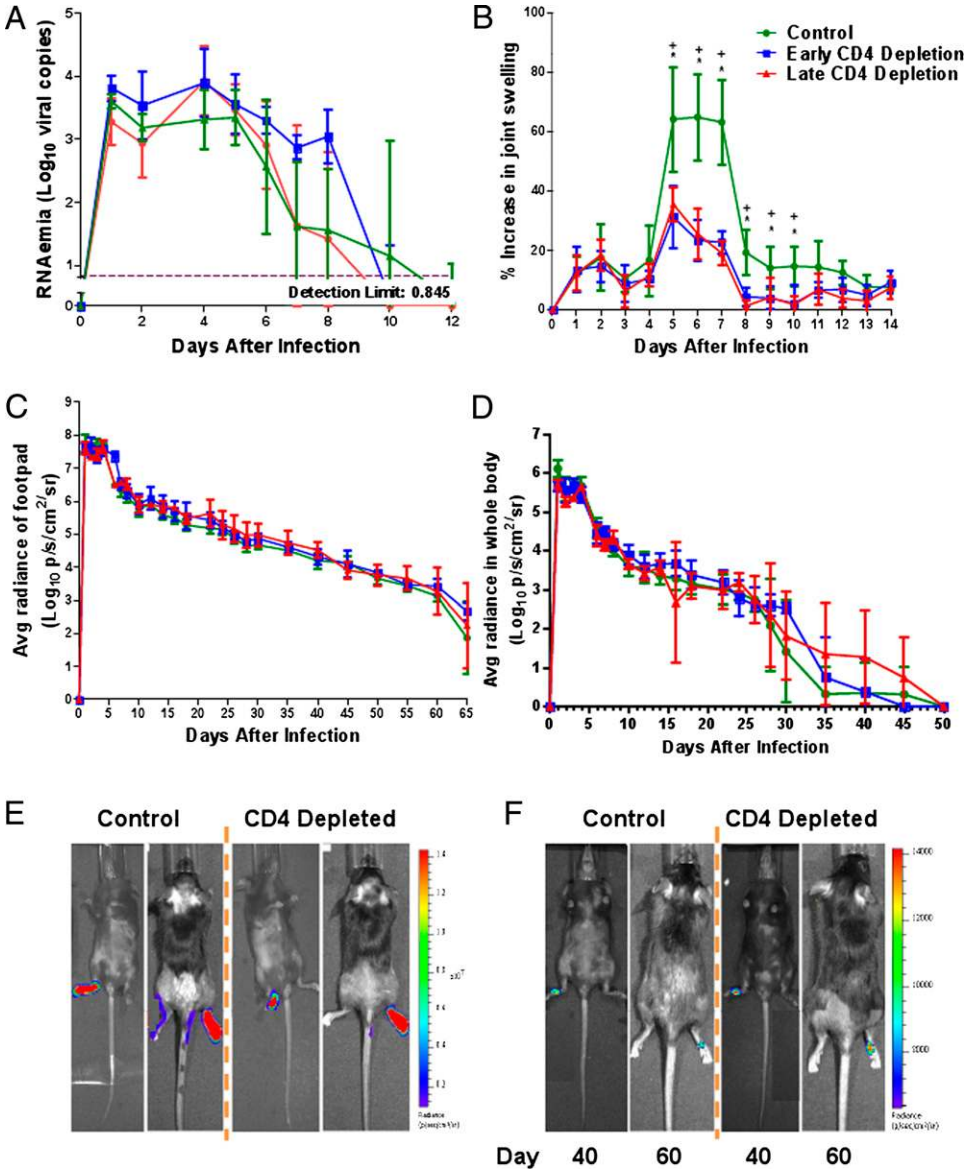

FIGURE 3. $CD4^+$ T cells mediate CHIKV-induced joint inflammation. RNAemia (**A**), percentage increase in joint swelling (**B**), average footpad bioluminescence reading (**C**), and average whole body bioluminescence reading (**D**) in control, early CD4 depletion, and late CD4 depletion groups ($n = 5$/group). (**E**) Representative pseudocolor images of whole body from control and early CD4 depletion groups on 1 dpi. (**F**) Representative pseudocolor images of whole body from control and early CD4 depletion groups on 40 dpi (FOV-D) and 60 dpi (FOV-C). All groups were infected with CHIKV LR2006-OPY1-Fluc. The early CD4 depletion group was given anti-CD4 Abs on −1 and 4 dpi, whereas the late CD4 depletion group was given anti-CD4 Abs only on 4 dpi. Monitoring was terminated when bioluminescence signals were no longer detectable. $^*p < 0.05$, early CD4 depletion versus control, $^+p < 0.05$, late CD4 depletion versus control, Kruskal–Wallis test followed by the Dunn test.

joints during the peak of swelling at 6 dpi. Phenotyping and quantification of $CD45^+$ leukocytes revealed an increase in $CD45^+$ cell numbers in the swollen joints (data not shown). $CD4^+$ and $CD8^+$ T cells were shown to increase in numbers (Fig. 5A, 5B), confirming previous reports that CHIKV infection could induce the recruitment of these leukocyte subsets to the joint (24, 27). Interestingly, depletion of $CD4^+$ T cells 24 h before joint extraction revealed that these cells partially control the recruitment of $CD8^+$ T cells to the joint. However, they have no effect on monocyte/macrophage or neutrophil ($CD45^+/CD11b^+/Ly6G^-$) recruitment, even though they were, by far, the most numerous populations (Fig. 5C, 5D).

To demonstrate that T cells, and in particular $CD4^+$ T cells, were specific for CHIKV, we next performed ELISPOT assays using whole CHIKV particles as Ags. Naive spleen cells were added to joint cells to provide sufficient numbers of APCs that might be missing in the joint cell population. High levels of IFN-γ–producing cells were detected at 6 dpi in the swollen joint of CHIKV-infected mice; however, similar levels were also detected in the absence of in vitro restimulation with CHIKV (Fig. 6A). This could be due to the presence of high virus titer in the footpad at 6 dpi (Figs. 3C, 4C), as well as the possible existence of CHIKV Ag–loaded APCs among the extracted footpad cells that could still trigger IFN-γ production by T cells during the in vitro incubation period. In vivo depletion of $CD4^+$ T cells strongly reduced the numbers of IFN-γ–producing cells in the joints (Fig. 6A), suggesting that this subset was the main producer of IFN-γ. However, based on this experiment it was not possible to exclude that depletion of $CD4^+$ T cells led to a reduction in the accumulation of other cells, such as $CD8^+$ T, NK, or NKT cells, which are also able to produce IFN-γ. In vivo depletion of $CD4^+$ partially reduced $CD8^+$ T cell numbers (Fig. 5B), but it had no effect on the number of NK or NKT cells in the joints (data not shown). Thus, the possibility that $CD8^+$ T cells were the major producer of IFN-γ could not be excluded. Therefore, we performed an additional experiment in which purified joint cells were depleted of $CD4^+$ T cells using a MACS column loaded with anti-CD4 Abs coupled with beads. After ex vivo depletion, the numbers of IFN-γ–producing cells in the joints of CHIKV-infected mice were reduced significantly. From this experiment, we could determine that $CD4^+$ T cells accounted for ∼50% of the IFN-γ–producing cells at 6 dpi (Fig. 6B).

ELISPOT assays were also repeated with cells isolated from the feet of recovered WT and $CD4^{-/-}$ mice at 93 dpi to determine whether CHIKV-specific memory $CD4^+$ and $CD8^+$ T cells remained

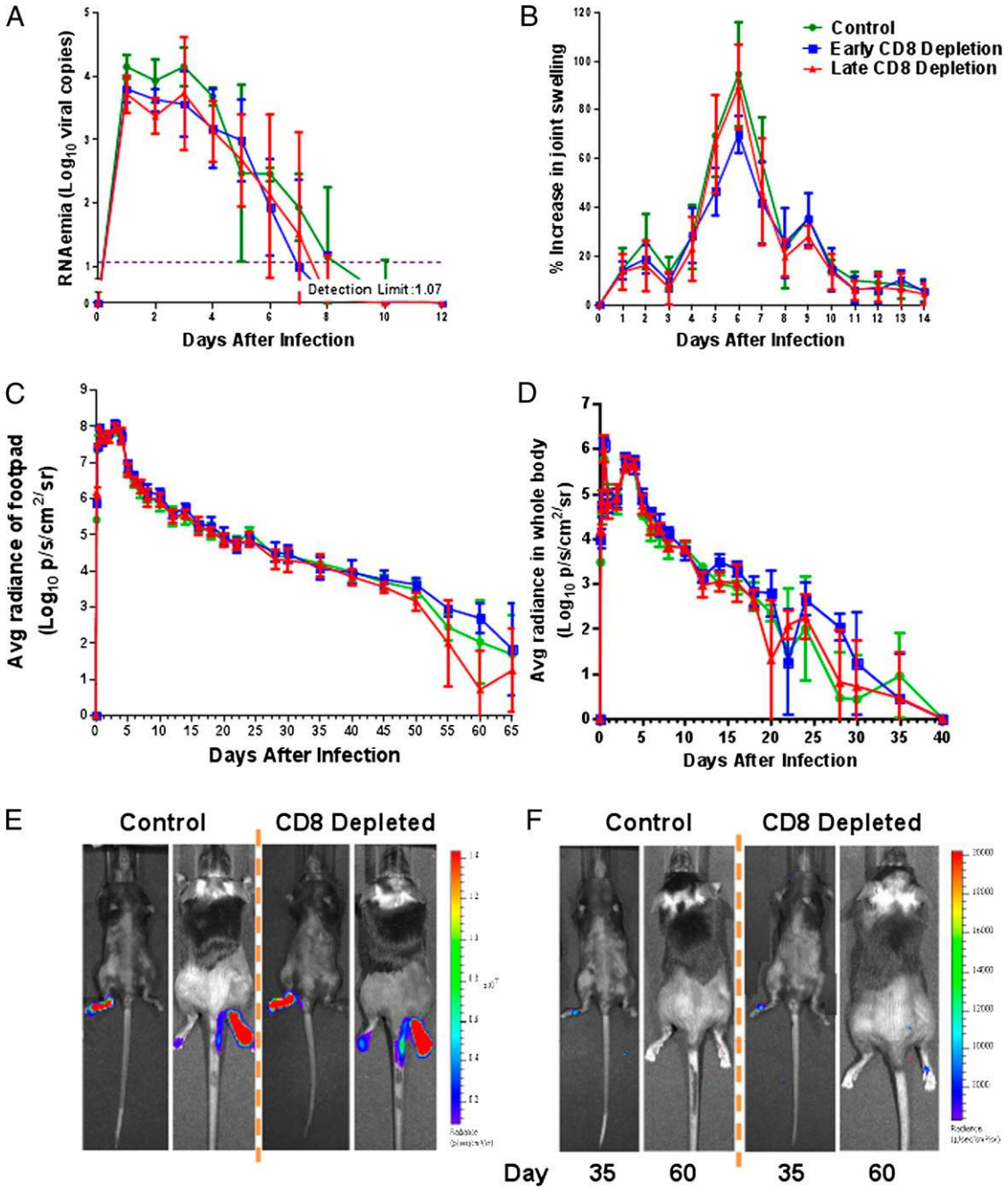

FIGURE 4. $CD8^+$ T cells have no role during CHIKV infection in C57BL/6J mice. RNAemia (**A**), percentage increase in joint swelling (**B**), average footpad bioluminescence reading (**C**), and average whole body bioluminescence reading (**D**) in control, early CD8 depletion, and late CD8 depletion groups ($n = 5$/group). (**E**) Representative pseudocolor images of whole body from control and CD8 early depletion groups on 1 dpi. (**F**) Representative pseudocolor images of whole body from control and early CD8 depletion groups on 35 dpi (FOV-D) and 60 dpi (FOV-C). All groups were infected with CHIKV LR2006-OPY1-Fluc. The early CD8 depletion group was given anti-CD8 Abs on −1 and 4 dpi, whereas the late CD8 depletion group received anti-CD8 Abs only on 4 dpi. Monitoring was terminated when bioluminescence signals were no longer detectable.

in the infected tissues. Overall, a significant reduction in IFN-γ–producing T cells was observed in these recovered footpads (Fig. 6C) compared with the footpads isolated from mice during the peak of joint swelling (Fig. 6A). However, the amount of IFN-γ–producing T cells in the footpads of recovered WT mice was significantly elevated upon in vitro restimulation with SGP11 CHIKV virions (Fig. 6C). Meanwhile, the absence of $CD4^+$ T cells significantly reduced the total number of IFN-γ–producing memory T cells (Fig. 6C). Taken together, these data demonstrated the presence of CHIKV-specific memory T cells in the footpads of infected mice that may persist in the joint after virus disappearance.

Induction of CHIKV-specific $CD4^+$ T cells in the spleen of acute infected mice

CHIKV infection did not induce splenomegaly or cause an increase in total splenocyte numbers (data not shown). Interesting, unlike in the joints, the increase in total $CD4^+$ and $CD8^+$ T cells in the spleen was not significant at 6 dpi (Fig. 7A, 7B). In addition, NK cell ($CD45^+$/$CD3^-$/$NK1.1^+$), NKT cell ($CD45^+$/$CD3^+$/$NK1.1^+$), monocyte/macrophage, and neutrophil numbers were not significantly different from those of naive mice during a CHIKV infection, although $CD4^+$ T cell depletion 24 h before spleen removal increased the numbers of NKT cells and monocytes/macrophages significantly (Fig. 7C–F).

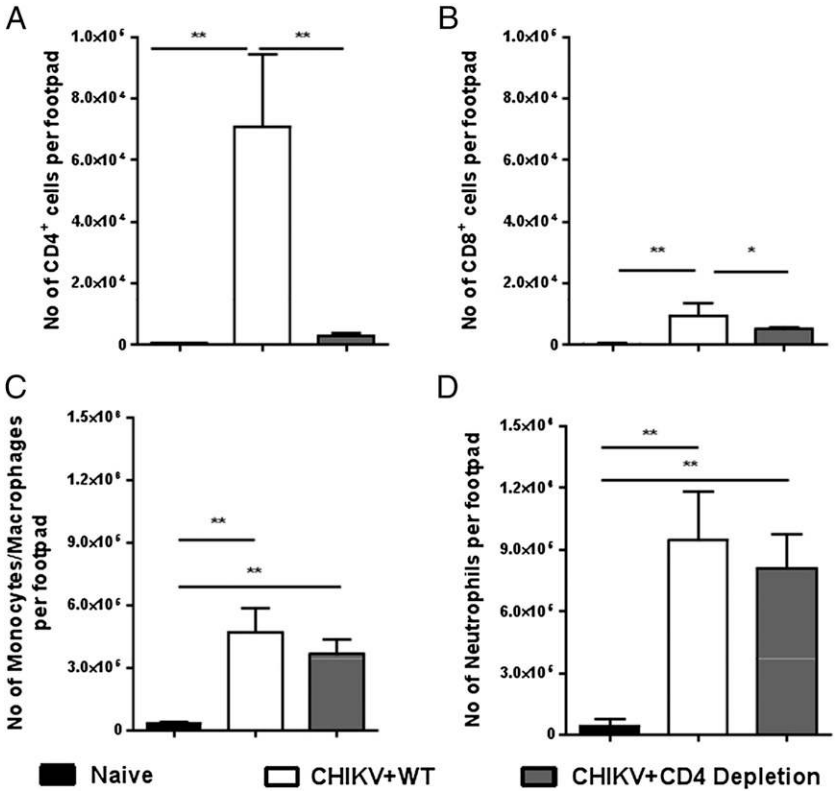

FIGURE 5. Induction of $CD4^+$ and $CD8^+$ T cells in footpad of mice with acute CHIKV infection. Average number of $CD4^+$ T cells (**A**), $CD8^+$ T cells (**B**), monocytes/macrophages (**C**), and neutrophils (**D**) per footpad in naive ($n = 5$), CHIKV+WT ($n = 5$), and CHIKV-infected and CD4-depleted (CHIKV+ CD4 depletion) ($n = 4$) mice on 6 dpi. CD4 depletion was done with injection of anti-CD4 Abs on 5 dpi. SGP11 isolate was used. $*p < 0.05$, $**p < 0.01$, one-way ANOVA followed by the Tukey multiple-comparison test.

An IFN-γ ELISPOT assay was performed to determine the presence of CHIKV-specific T cells in the spleen during acute infection (6 dpi). A substantial number of CHKV-specific IFN-γ–producing T cells was detected only after ex vivo restimulation with SGP11 virions (Fig. 6D). These data suggest that, contrary to the joints, there are very few CHIKV-infected cells in the spleen that are able to present viral Ags to T cells at 6 dpi. However, similar to the joints, both in vivo and ex vivo $CD4^+$ T cell depletion demonstrated that $CD4^+$ T cells represent the main subset (~90%) of IFN-γ–producing cells in the spleen during the acute phase of the infection (Fig. 6D, 6E).

$CD4^+$ T cells mediate joint swelling independently of IFN-γ

Because CHIKV-specific $CD4^+$ T cells could be demonstrated by IFN-γ ELISPOT assay in the joint of infected mice, we next investigated whether this cytokine could be involved in joint swelling. IFN-$\gamma^{-/-}$ mice were infected with CHIKV SGP11, and RNAemia and joint swelling were monitored. RNAemia was significantly higher in the IFN-$\gamma^{-/-}$ mice from 4 to 8 dpi (Fig. 8A). More importantly, IFN-$\gamma^{-/-}$ mice had more pronounced joint swelling at 5 dpi (Fig. 8B), clearly indicating that IFN-γ is not the main factor mediating CHIKV-induced joint pathology.

Discussion

The role of T cells in the pathogenesis of CHIKV disease is largely undefined. In this study, we demonstrated that CHIKV-specific $CD4^+$ T cells are the major mediator of inflammation in the footpad of CHIKV-infected mice.

The first hint of T cell involvement in the pathogenesis of CHIKV infection was observed in acute CHIKV-infected patients; activated $CD4^+$ and $CD8^+$ T cells were significantly elevated in peripheral blood cells compared with healthy controls (25). Further studies on CHIKV-infected patients performed to define peripheral blood T cell responses that occurred during acute CHIKV infection revealed an early-stage proliferation and activation of $CD8^+$ T cells, whereas the later stage of the acute phase was characterized by a switch to $CD4^+$ T cell responses (26). These observations support the hypothesis of an early antiviral cytotoxic $CD8^+$ response to control virus replication, followed by a switch to $CD4^+$ T cell responses to facilitate neutralizing Ab production.

To our knowledge, in this study, we first showed that T cells are not required to control virus replication, which differs from the responses observed in viruses, such as HIV (31), and other arthritogenic viruses, such as Ross River virus (32). Experiments using RAG2$^{-/-}$ mice lacking both T and B cells, as well as T cell subset-deficient mice, clearly demonstrated a crucial role for humoral responses. Surprisingly, the controlled viremia observed in CD4$^{-/-}$ mice demonstrated the importance of $CD4^+$ Th-independent Ab responses in limiting virus replication. In RAG2$^{-/-}$ mice, CHIKV established a chronic infection with a high level of circulating viruses. However, none of these mice died of CHIKV infection, even out to 40 dpi. Using bioluminescent imaging, we also observed that CHIKV persisted in the joint for ≥60 d in WT mice. However, the absence or depletion of either type of T cells did not modify virus replication or persistence in the joint. Effectively, these data strongly imply that innate immune cells, such as NK or dendritic cells, acting directly or via antiviral cytokine release may partially control virus replication. More work is needed to identify these immune responses.

CHIKV-induced joint inflammation was reported previously not to correlate directly with viremia in mice (24, 27). Instead, the peak of joint swelling occurs shortly after a rapid virus clearance at 4 dpi, suggesting that inflammation is largely mediated by a pathogenic immune response. Our data showed that the absence of $CD4^+$, but not $CD8^+$, T cells during the course of CHIKV inflection significantly reduced joint swelling and tissue damage in the joints. Thus, $CD4^+$ T cells mediated their effect locally, because their numbers were significantly elevated in the joints during the peak of inflammation at 6 dpi. Moreover, we also showed by ELISPOT that a significant proportion of CHIKV-specific activated $CD4^+$

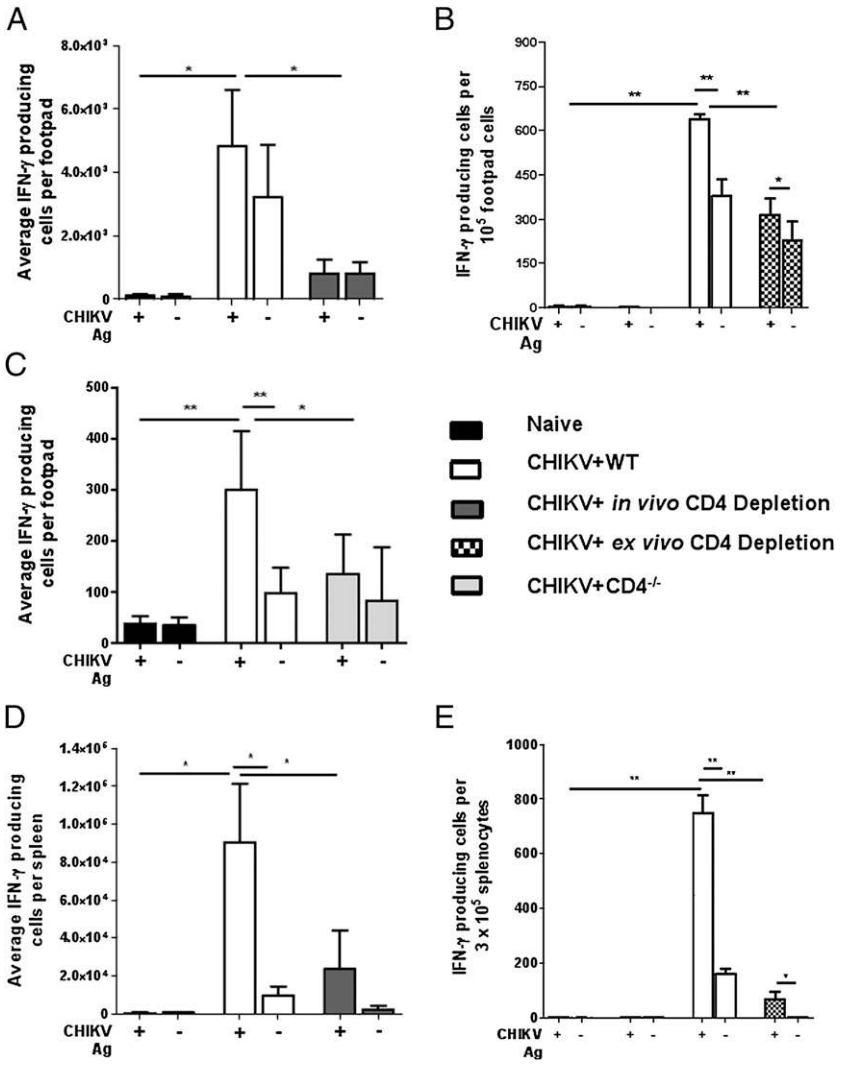

FIGURE 6. Induction of CHIKV-specific T cells during CHIKV infection. The number of IFN-γ–producing cells in the footpad of acute infected mice with in vivo $CD4^+$ T cell depletion (6 dpi) (**A**), acute infected mice with ex vivo $CD4^+$ T cell depletion (6 dpi) (**B**), and mice that recovered from infection (93 dpi) (**C**) (n = 5/group) were detected by ELISPOT. The number of IFN-γ–producing cells in spleens of acute infected mice with in vivo $CD4^+$ T cell depletion (6 dpi) (**D**) and acute infected mice with ex vivo $CD4^+$ T cell depletion (6 dpi) (**E**) (n = 5/group). For ex vivo CD4 depletion, ELISPOT was done in pooled samples of five mice/group in replicates of five. SGP11 isolate was used. $^*p < 0.05$, $^{**}p < 0.01$, one-way ANOVA followed by the Tukey multiple-comparison test.

T cells were present in both the joint and in the spleen of infected animals at 6 dpi. These data demonstrated a rapid expansion of CHIKV-specific $CD4^+$ T cells induced by CHIKV infection. Although it is not clear where these cells are primed, a fraction of CHIKV-specific naive T cells could be primed in the lymph node draining the site of virus inoculation, whereas another fraction could be primed in the spleen. Future experiments are needed to clarify this phenomenon.

The depletion data described in this study clearly suggest that $CD4^+$ T cells are directly responsible for joint sγwelling. Although the number of $CD8^+$ T cells in the joint was reduced after depletion of $CD4^+$ T cells, additional experiments (see above) ruled out a role for the $CD8^+$ subset in joint swelling. Intriguingly, the depletion of $CD4^+$ T cells had no effect on monocyte/macrophage or neutrophil migration to the joint (Fig. 5), because monocytes/macrophages have been incriminated as a mediator of joint pathology during infection (24). There, monocytes/macrophages were depleted using the clodronate/liposome method on the same day that CHIKV infection was initiated (24). Nevertheless, clodronate treatment was also shown to deplete all phagocytic cells, including dendritic cells (33, 34). Because dendritic cells are crucial for $CD4^+$ T cell priming, it is plausible that clodronate treatment prevented the induction of pathogenic $CD4^+$ T cells. Future studies are required to define the exact roles of these different subsets in CHIKV-induced pathology.

Although the mechanism by which CHIKV-specific $CD4^+$ T cells mediate joint pathology remains elusive, the current knowledge of cytokine and chemokine profiles during CHIKV infection suggests that $CD4^+$ T cells could mediate inflammation via Th17- and Th1-related mechanisms as observed in rheumatoid arthritis (35). Elevated Th17-associated cytokines, such as IL-1β, IL-6, and IL-17, were reported in humans and in CHIKV mouse models (24, 26, 36–40). Studies from patient cohorts also reported elevated levels of Th1-associated cytokines, such as IFN-γ, TNF-α, IL-12, IL-15, and IL-18, and chemokines, such as IP-10, Mig, MIP-1α, and MIP-1β, during CHIKV infection (25, 26, 36–39, 41, 42). In CHIKV-infected mice, Th1 cytokines, such as IFN-γ and TNF-α, from both sera (40) and inflamed tissues (24) were elevated during the inflammatory phase. Unexpectedly, Th1-stimulating cytokines, such as IL-12, IL-15, and IL-18, were elevated before the inflammatory phase (40), suggesting an expansion of Th1-lineage $CD4^+$ T cells before the induction of inflammation. Elevated IFN-γ observed during the peak of inflammation was preceded by increased levels of IL-12p35 and IL-18 in the inflamed footpad (T.H. Hui, L. Rénia, and L. Ng, unpublished observations). In this study, we showed that CHIKV-specific T cells producing IFN-γ are present in the joint, suggesting a possible role for IFN-γ in joint pathology. Infections in IFN-$\gamma^{-/-}$ mice demonstrated that IFN-γ is not a proinflammatory mediator of joint swelling during CHIKV SGP11 infection (Fig. 8), contrasting with a recent study

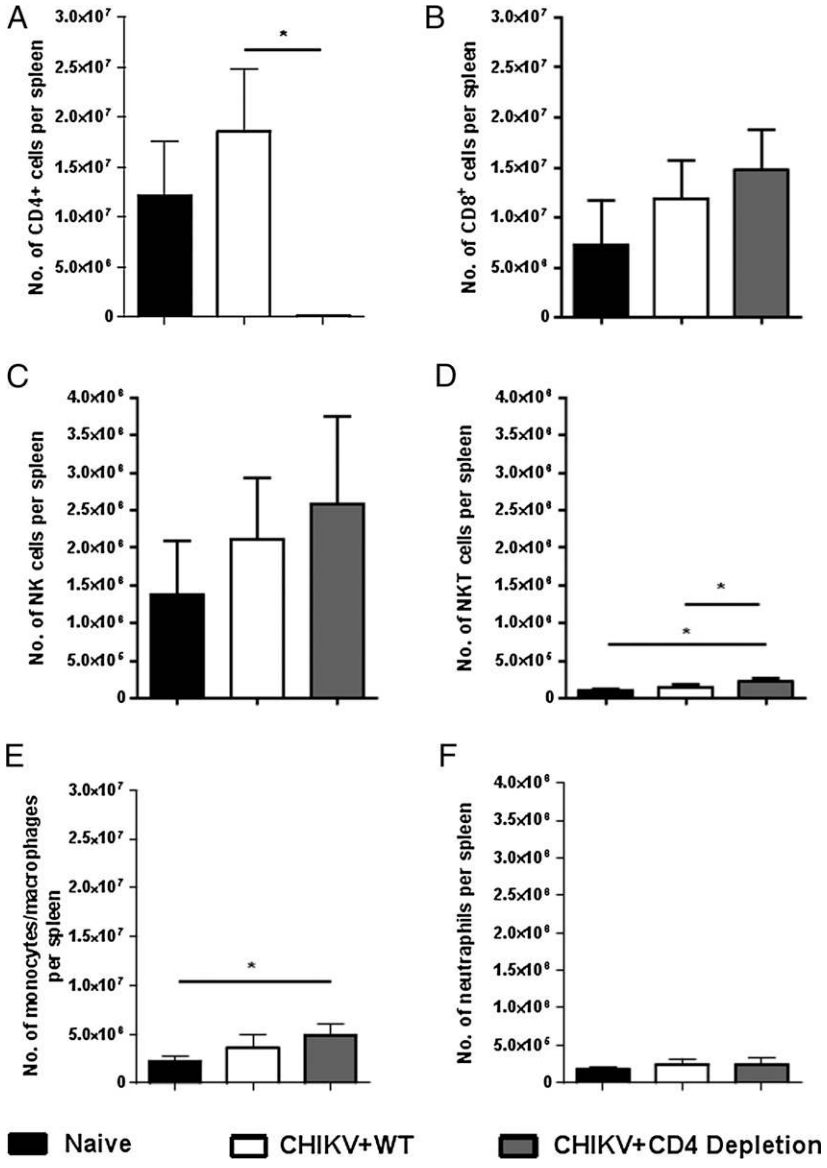

FIGURE 7. Leukocyte profiling in the spleen during acute CHIKV infection. Number of $CD4^+$ T cells (**A**), $CD8^+$ T cells (**B**), NK cells (**C**), NKT cells (**D**), monocytes/macrophages (**E**), and neutrophils (**F**) per spleen in naive ($n = 5$), CHIKV+WT ($n = 5$), and CHIKV+CD4 depletion ($n = 4$) groups on 6 dpi. CD4 depletion was done by injecting anti-CD4 Abs on 5 dpi. SGP11 isolate was used. $*p < 0.05$, one-way ANOVA followed by the Tukey multiple-comparison test.

using IFN-$\gamma^{-/-}$ mice (43). This difference in disease severity observed could be due to the different virus isolates that were used, implying that $CD4^+$ T cells may mediate joint swelling by different mechanisms.

The role of T cells in the pathogenesis of alphaviruses is highly varied. It was demonstrated in murine Venezuelan equine encephalitis virus infection that the early influx of $CD3^+$ T cells confers protection (44), and both $CD4^+$ and $CD8^+$ cells were shown to have direct antiviral effects in the CNS (45). Likewise, T cells are involved both as mediators of neuropathology and virus clearance in murine Sindbis virus infections (46, 47). Additionally, it was found that $CD4^+$ T cells mediated fatal encephalitis through IFN-γ production (46), as well as hippocampus damage through mononuclear cell recruitment during Sindbis virus in-

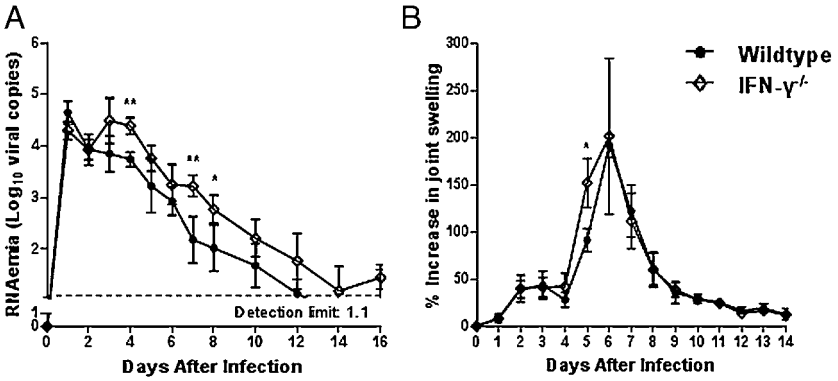

FIGURE 8. RNAemia and joint swelling in CHIKV-infected IFN-$\gamma^{-/-}$ mice. RNAemia (**A**) and percentage increase in joint swelling (**B**) in WT ($n = 5$) and IFN-$\gamma^{-/-}$ ($n = 5$) mice; RNAemia monitoring was terminated at 14 dpi. All groups were infected with CHIKV SGP11. Detection limits of RNAemia were determined by average signals from blood of mock-infected mice ($n = 2$). $*p < 0.05$, $**p < 0.01$, Mann–Whitney U test.

fection (48). Pathogenic T cells were also shown to generate lesions of demyelination in murine Semliki Forest virus infection (49), and depletion of $CD8^+$ T cells reduced demyelination (50), whereas depletion of $CD4^+$ T cells only reduced the extent of the inflammation (49). The data presented in this study are similar to those for both Sindbis virus and Semliki Forest virus infections, in which $CD4^+$ T cells clearly play a pathogenic role. Nevertheless, macrophages, and not T cells, are involved in joint pathology in Ross River virus infections (32).

Although peripheral T cells in patients displayed an activated profile by flow cytometry during CHIKV infection (25, 26), these studies are inadequate to establish the functional roles of T cells in CHIKV-induced pathology. Future studies should be extended to human cohorts to identify CHIKV-specific T cell populations in peripheral blood cells and synovial extracts during the symptomatic phase.

Acknowledgments

We thank Marjorie Mauduit (Singapore Immunology Network), Zhisheng Her (Singapore Immunology Network), and Age Utt (University of Tartu) for technical assistance.

Disclosures

The authors have no financial conflicts of interest.

References

1. Powers, A. M., and C. H. Logue. 2007. Changing patterns of chikungunya virus: re-emergence of a zoonotic arbovirus. *J. Gen. Virol.* 88: 2363–2377.
2. Renault, P., J. L. Solet, D. Sissoko, E. Balleydier, S. Larrieu, L. Filleul, C. Lassalle, J. Thiria, E. Rachou, H. de Valk, et al. 2007. A major epidemic of chikungunya virus infection on Reunion Island, France, 2005-2006. *Am. J. Trop. Med. Hyg.* 77: 727–731.
3. Sergon, K., A. A. Yahaya, J. Brown, S. A. Bedja, M. Mlindasse, N. Agata, Y. Allaranger, M. D. Ball, A. M. Powers, V. Ofula, et al. 2007. Seroprevalence of Chikungunya virus infection on Grande Comore Island, union of the Comoros, 2005. *Am. J. Trop. Med. Hyg.* 76: 1189–1193.
4. Ravi, V. 2006. Re-emergence of chikungunya virus in India. *Indian J. Med. Microbiol.* 24: 83–84.
5. Thiboutot, M. M., S. Kannan, O. U. Kawalekar, D. J. Shedlock, A. S. Khan, G. Sarangan, P. Srikanth, D. B. Weiner, and K. Muthumani. 2010. Chikungunya: a potentially emerging epidemic? *PLoS Negl. Trop. Dis.* 4: e623.
6. Renault, P., E. Balleydier, E. D'Ortenzio, M. Bâville, and L. Filleul. 2012. Epidemiology of Chikungunya infection on Reunion Island, Mayotte, and neighboring countries. *Med. Mal. Infect.* 42: 93–101.
7. Chua, K. B. 2010. Epidemiology of chikungunya in Malaysia: 2006-2009. *Med. J. Malaysia* 65: 277–282.
8. Her, Z., Y. W. Kam, R. T. Lin, and L. F. Ng. 2009. Chikungunya: a bending reality. *Microbes Infect.* 11: 1165–1176.
9. Robinson, M. C. 1955. An epidemic of virus disease in Southern Province, Tanganyika Territory, in 1952-53. I. Clinical features. *Trans. R. Soc. Trop. Med. Hyg.* 49: 28–32.
10. Borgherini, G., P. Poubeau, F. Staikowsky, M. Lory, N. Le Moullec, J. P. Becquart, C. Wengling, A. Michault, and F. Paganin. 2007. Outbreak of chikungunya on Reunion Island: early clinical and laboratory features in 157 adult patients. *Clin. Infect. Dis.* 44: 1401–1407.
11. Lakshmi, V., M. Neeraja, M. V. Subbalaxmi, M. M. Parida, P. K. Dash, S. R. Santhosh, and P. V. Rao. 2008. Clinical features and molecular diagnosis of Chikungunya fever from South India. *Clin. Infect. Dis.* 46: 1436–1442.
12. Solanski, B. S., S. C. Arya, and P. Maheshwari. 2007. Chikungunya disease with nephritic presentation. *Int. J. Clin. Pract.* 61: 1941.
13. Mirabel, M., O. Vignaux, P. Lebon, P. Legmann, S. Weber, and C. Meune. 2007. Acute myocarditis due to Chikungunya virus assessed by contrast-enhanced MRI. *Int. J. Cardiol.* 121: e7–e8.
14. Simon, F., P. Paule, and M. Oliver. 2008. Chikungunya virus-induced myopericarditis: toward an increase of dilated cardiomyopathy in countries with epidemics? *Am. J. Trop. Med. Hyg.* 78: 212–213.
15. Mittal, A., S. Mittal, M. J. Bharati, R. Ramakrishnan, S. Saravanan, and P. S. Sathe. 2007. Optic neuritis associated with chikungunya virus infection in South India. *Arch. Ophthalmol.* 125: 1381–1386.
16. Chandak, N. H., R. S. Kashyap, D. Kabra, P. Karandikar, S. S. Saha, S. H. Morey, H. J. Purohit, G. M. Taori, and H. F. Daginawala. 2009. Neurological complications of Chikungunya virus infection. *Neurol. India* 57: 177–180.
17. Ganesan, K., A. Diwan, S. K. Shankar, S. B. Desai, G. S. Sainani, and S. M. Katrak. 2008. Chikungunya encephalomyeloradiculitis: report of 2 cases with neuroimaging and 1 case with autopsy findings. *AJNR Am. J. Neuroradiol.* 29: 1636–1637.
18. Couderc, T., F. Chrétien, C. Schilte, O. Disson, M. Brigitte, F. Guivel-Benhassine, Y. Touret, G. Barau, N. Cayet, I. Schuffenecker, et al. 2008. A mouse model for Chikungunya: young age and inefficient type-I interferon signaling are risk factors for severe disease. *PLoS Pathog.* 4: e29.
19. Schilte, C., T. Couderc, F. Chretien, M. Sourisseau, N. Gangneux, F. Guivel-Benhassine, A. Kraxner, J. Tschopp, S. Higgs, A. Michault, et al. 2010. Type I IFN controls chikungunya virus via its action on nonhematopoietic cells. *J. Exp. Med.* 207: 429–442.
20. Labadie, K., T. Larcher, C. Joubert, A. Mannioui, B. Delache, P. Brochard, L. Guigand, L. Dubreil, P. Lebon, B. Verrier, et al. 2010. Chikungunya disease in nonhuman primates involves long-term viral persistence in macrophages. *J. Clin. Invest.* 120: 894–906.
21. Her, Z., B. Malleret, M. Chan, E. K. Ong, S. C. Wong, D. J. Kwek, H. Tolou, R. T. Lin, P. A. Tambyah, L. Rénia, and L. F. Ng. 2010. Active infection of human blood monocytes by Chikungunya virus triggers an innate immune response. *J. Immunol.* 184: 5903–5913.
22. Werneke, S. W., C. Schilte, A. Rohatgi, K. J. Monte, A. Michault, F. Arenzana-Seisdedos, D. L. Vanlandingham, S. Higgs, A. Fontanet, M. L. Albert, and D. J. Lenschow. 2011. ISG15 is critical in the control of Chikungunya virus infection independent of UbE1L mediated conjugation. *PLoS Pathog.* 7: e1002322.
23. Gardner, C. L., C. W. Burke, S. T. Higgs, W. B. Klimstra, and K. D. Ryman. 2012. Interferon-alpha/beta deficiency greatly exacerbates arthritogenic disease in mice infected with wild-type chikungunya virus but not with the cell culture-adapted live-attenuated 181/25 vaccine candidate. *Virology* 425: 103–112.
24. Gardner, J., I. Anraku, T. T. Le, T. Larcher, L. Major, P. Roques, W. A. Schroder, S. Higgs, and A. Suhrbier. 2010. Chikungunya virus arthritis in adult wild-type mice. *J. Virol.* 84: 8021–8032.
25. Hoarau, J. J., M. C. Jaffar Bandjee, P. Krejbich Trotot, T. Das, G. Li-Pat-Yuen, B. Dassa, M. Denizot, E. Guichard, A. Ribera, T. Henni, et al. 2010. Persistent chronic inflammation and infection by Chikungunya arthritogenic alphavirus in spite of a robust host immune response. *J. Immunol.* 184: 5914–5927.
26. Wauquier, N., P. Becquart, D. Nkoghe, C. Padilla, A. Ndjoyi-Mbiguino, and E. M. Leroy. 2011. The acute phase of Chikungunya virus infection in humans is associated with strong innate immunity and T CD8 cell activation. *J. Infect. Dis.* 204: 115–123.
27. Morrison, T. E., L. Oko, S. A. Montgomery, A. C. Whitmore, A. R. Lotstein, B. M. Gunn, S. A. Elmore, and M. T. Heise. 2011. A mouse model of chikungunya virus-induced musculoskeletal inflammatory disease: evidence of arthritis, tenosynovitis, myositis, and persistence. *Am. J. Pathol.* 178: 32–40.
28. Kam, Y. W., F. M. Lum, T. H. Teo, W. W. Lee, D. Simarmata, S. Harjanto, C. L. Chua, Y. F. Chan, J. K. Wee, A. Chow, et al. 2012. Early neutralizing IgG response to Chikungunya virus in infected patients targets a dominant linear epitope on the E2 glycoprotein. *EMBO Mol Med* 4: 330–343.
29. Pohjala, L., A. Utt, M. Varjak, A. Lulla, A. Merits, T. Ahola, and P. Tammela. 2011. Inhibitors of alphavirus entry and replication identified with a stable Chikungunya replicon cell line and virus-based assays. *PLoS ONE* 6: e28923.
30. Tsetsarkin, K., S. Higgs, C. E. McGee, X. De Lamballerie, R. N. Charrel, and D. L. Vanlandingham. 2006. Infectious clones of Chikungunya virus (La Réunion isolate) for vector competence studies. *Vector Borne Zoonotic Dis.* 6: 325–337.
31. Migueles, S. A., C. M. Osborne, C. Royce, A. A. Compton, R. P. Joshi, K. A. Weeks, J. E. Rood, A. M. Berkley, J. B. Sacha, N. A. Cogliano-Shutta, et al. 2008. Lytic granule loading of $CD8^+$ T cells is required for HIV-infected cell elimination associated with immune control. *Immunity* 29: 1009–1021.
32. Morrison, T. E., A. C. Whitmore, R. S. Shabman, B. A. Lidbury, S. Mahalingam, and M. T. Heise. 2006. Characterization of Ross River virus tropism and virus-induced inflammation in a mouse model of viral arthritis and myositis. *J. Virol.* 80: 737–749.
33. Zhang, Y., W. D. Shlomchik, G. Joe, J. P. Louboutin, J. Zhu, A. Rivera, D. Giannola, and S. G. Emerson. 2002. APCs in the liver and spleen recruit activated allogeneic $CD8^+$ T cells to elicit hepatic graft-versus-host disease. *J. Immunol.* 169: 7111–7118.
34. Hashimoto, D., A. Chow, M. Greter, Y. Saenger, W. H. Kwan, M. Leboeuf, F. Ginhoux, J. C. Ochando, Y. Kunisaki, N. van Rooijen, et al. 2011. Pretransplant CSF-1 therapy expands recipient macrophages and ameliorates GVHD after allogeneic hematopoietic cell transplantation. *J. Exp. Med.* 208: 1069–1082.
35. Komatsu, N., and H. Takayanagi. 2012. Inflammation and bone destruction in arthritis: synergistic activity of immune and mesenchymal cells in joints. *Front Immunol* 3: 77.
36. Ng, L. F., A. Chow, Y. J. Sun, D. J. Kwek, P. L. Lim, F. Dimatatac, L. C. Ng, E. E. Ooi, K. H. Choo, Z. Her, et al. 2009. IL-1beta, IL-6, and RANTES as biomarkers of Chikungunya severity. *PLoS ONE* 4: e4261.
37. Chow, A., Z. S. Her, E. K. Ong, J. M. Chen, F. Dimatatac, D. J. Kwek, T. Barkham, H. Yang, L. Rénia, Y. S. Leo, and L. F. Ng. 2011. Persistent arthralgia induced by Chikungunya virus infection is associated with interleukin-6 and granulocyte macrophage colony-stimulating factor. *J. Infect. Dis.* 203: 149–157.
38. Lee, N., C. K. Wong, W. Y. Lam, A. Wong, W. Lim, C. W. Lam, C. S. Cockram, J. J. Sung, P. K. Chan, and J. W. Tang. 2006. Chikungunya fever, Hong Kong. *Emerg. Infect. Dis.* 12: 1790–1792.
39. Chaaitanya, I. K., N. Muruganandam, S. G. Sundaram, O. Kawalekar, A. P. Sugunan, S. P. Manimunda, S. R. Ghosal, K. Muthumani, and P. Vijayachari. 2011. Role of proinflammatory cytokines and chemokines in chronic arthropathy in CHIKV infection. *Viral Immunol.* 24: 265–271.
40. Chirathaworn, C., P. Rianthavorn, N. Wuttirattanakowit, and Y. Poovorawan. 2010. Serum IL-18 and IL-18BP levels in patients with Chikungunya virus infection. *Viral Immunol.* 23: 113–117.

41. Kelvin, A. A., D. Banner, G. Silvi, M. L. Moro, N. Spataro, P. Gaibani, F. Cavrini, A. Pierro, G. Rossini, M. J. Cameron, et al. 2011. Inflammatory cytokine expression is associated with chikungunya virus resolution and symptom severity. *PLoS Negl. Trop. Dis.* 5: e1279.
42. Patil, D. R., S. L. Hundekar, and V. A. Arankalle. 2012. Expression profile of immune response genes during acute myopathy induced by chikungunya virus in a mouse model. *Microbes Infect.* 14: 457–469.
43. Nakaya, H. I., J. Gardner, Y. S. Poo, L. Major, B. Pulendran, and A. Suhrbier. 2012. Gene profiling of chikungunya virus arthritis reveals significant overlap with rheumatoid arthritis. *Arthritis Rheum.* 10.1002/art.34631.
44. Yun, N. E., B. H. Peng, A. S. Bertke, V. Borisevich, J. K. Smith, J. N. Smith, A. L. Poussard, M. Salazar, B. M. Judy, M. A. Zacks, et al. 2009. $CD4^+$ T cells provide protection against acute lethal encephalitis caused by Venezuelan equine encephalitis virus. *Vaccine* 27: 4064–4073.
45. Brooke, C. B., D. J. Deming, A. C. Whitmore, L. J. White, and R. E. Johnston. 2010. T cells facilitate recovery from Venezuelan equine encephalitis virus-induced encephalomyelitis in the absence of antibody. *J. Virol.* 84: 4556–4568.
46. Rowell, J. F., and D. E. Griffin. 2002. Contribution of T cells to mortality in neurovirulent Sindbis virus encephalomyelitis. *J. Neuroimmunol.* 127: 106–114.
47. Griffin, D. E. 2010. Recovery from viral encephalomyelitis: immune-mediated noncytolytic virus clearance from neurons. *Immunol. Res.* 47: 123–133.
48. Kimura, T., and D. E. Griffin. 2003. Extensive immune-mediated hippocampal damage in mice surviving infection with neuroadapted Sindbis virus. *Virology* 311: 28–39.
49. Fazakerley, J. 2004. Semliki Forest virus infection of laboratory mice: a model to study the pathogenesis of viral encephalitis. In *Emergence and Control of Zoonotic Viral Encephalitides*, 1st Ed. C. H. Calisher, and D. E. Griffin, eds. Springer-Verlag, Berlin, p. 179–190.
50. Subak-Sharpe, I., H. Dyson, and J. Fazakerley. 1993. In vivo depletion of $CD8^+$ T cells prevents lesions of demyelination in Semliki Forest virus infection. *J. Virol.* 67: 7629–7633.